Numerical simulation of the performance of an asymmetrical airfoil under extreme weather conditions

Ibrahim Kipngeno Rotich[a,b]*, László E. Kollár[a]

[a] *ELTE, Faculty of Informatics, Savaria Institute of Technology*
[b] *ELTE, Faculty of Science, Doctoral School of Environmental Sciences*

ABSTRACT

This paper presents a numerical study of icing of a NACA2412 airfoil and the aerodynamic performance of the airfoil with ice accretion. The study analyzes the effects of liquid water content, accretion time and varying angles of attack (AoA) up to 20° on ice accretion and, consequently, on the aerodynamic coefficients of the airfoil. The free stream velocity and air temperature were kept constant in the simulations. Results revealed that the ratio of lift and drag coefficients was the highest after a short accretion time (i.e., about 20 minutes) for AoA up to 10°, but then it decreased significantly with accretion time. Ice accretion increased with time; its mass was the greatest at 10° of AoA. The results can be beneficial for designing blade shapes to optimize wind turbine performance during adverse weather conditions.

Keywords: *ice accretion, ice mass, aerodynamic performance, airfoil, LWC*

1. Introduction

Icing conditions pose a great danger in the power production of wind turbines, causing uncertainties in future power demand [1, 2]. Other associated impacts of icing include increased operation and maintenance costs, structural integrity disturbance, lifespan reduction of wind turbines and permanent stall of turbines [3–6]. The icing depends on parameters such as freestream velocity, temperature, liquid water content (LWC), and droplet size distribution (DSD). The temperature affects the icing rate and nature of ice (rime, glaze or mixed) formed on the surface. LWC determines water present in the icing domain showing the severity of icing, type and shape of ice. Droplet diameter influences the local collision efficiencies, icing rate and type of ice formed. The geometry of the airfoil, i.e., airfoil orientation, angle of attack and surface roughness, determines the accretion rate, while accretion time affects the ice shape and mass of ice. The combined effects of the thermodynamic parameters determine the icing intensity on the airfoil surface [7]. Small water droplets may have a temperature below 0° without freezing. When these supercooled water droplets hit the cold surface, they freeze upon impact to form the ice accretion. The process is called dry growth if there is no unfrozen water on the surface and it results in rime ice. When there is a liquid layer on the surface, then the process is called wet growth and it results in glaze ice.

Power loss is affected by the accretion's intensity, frequency and duration of icing events [8] estimated that 20% of power losses occurs annually due to icing [9]. Gao & Hu [10] studied the effect of icing on a utility-scale turbine for a period of 51 hrs yielding 25 MW power loss. Homola et al.

*Corresponding author: Ibrahim Kipngeno Rotich, ibrahimrkipp@gmail.com
https://doi.org/10.37775/EIS.2022.2.2

[11] simulated icing effect on NREL 5MW baseline turbine leading to 24-27% power loss. The need to reduce power loss has been in constant progress with several studies done. Icing controls using microwaves and other anti/de-icing techniques minimize the impact of icing, but their applicability is becoming a challenge due to costs and the amount of energy needed in heating [12–15]. Simulation of icing helps improve safety and maintenance, reduce power losses, and decrease the load on the blade, which can cause the delamination and fracturing of the blade and thus reducing the lifespan. Ice accretion on the blade over an extended period increases the airfoil's mass, and can cause power reduction of up to 80% [10]. The reduction in power production also depends on the frequency of icing events in the region [16]. Ice accretion on the surface is affected by the duration in which the icing occurs. In anti-icing and de-icing systems, the heating element is mostly installed on the leading edge where most ice accumulates [17], and the accretion on the leading edge is greatly affected by the angle of attack and accretion time.

Research on wind turbines and on the impacts of icing poses challenges with limited resources, such as the use of drones, and Supervisory Control and Data Acquisition (SCADA) was employed due to the complexity of identifying real-time icing on the blades [15]. Ice accumulation experiments on wind farms are costly and have operational difficulties; thus, the use of numerical simulations has increased compliance. The numerical approach conveniently provides information on aerodynamics and predicts energy production losses due to icing. A laboratory setup is applicable to estimate the amount of ice accretion after reproducing the icing conditions, assuming that conditions do not vary during the experiment. Numerical models on ice accretion involve complex flow simulation on the airfoil, boundary layer characteristics and water droplet behavior, and iced surface thermodynamics with phase changes. Softwares used for modeling wind turbine and aeronautical icing applications include TURBICE, FENSAP ICE, and LEWICE. Virk et al. [18] used TURBICE software to numerically simulate the effects of ice accretion near the tip on the NACA 64618 blade profile by varying the angle of attack from -5 to 7.5 °C. The airflow around the airfoil impacted the ice formation on the leading-edge surface with lower angle of attack having less ice. Kollar & Mishra [16] numerically studied the icing on wind turbine blade sections under adverse weather conditions with Matlab. Fu & Farzaneh [19] developed a computational fluid dynamics model on rime ice accretion on a 450-kW/S809 horizontal axis wind turbine. Hildebrandt & Sun [20] carried out a comparative numerical assessment on the impact of short icing events of five 2 hour scenarios with varied atmospheric conditions on a 1.5 MW turbine and compared the icing rate on stalled turbine and a rotating turbine using ANSYS FLUENT.

This study applies the numerical approach for modelling icing over a wind turbine blade section using FENSAP-ICE. The ice accretion on the bare and the iced blade is simulated, and the corresponding aerodynamic coefficients (lift and drag) and the loads of ice (mass) are compared. The results obtained provide information on the extent of aerodynamic degradation due to icing and disturbance of flow over the airfoil by accreted ice. The results will help determine airfoil shape with minimal ice accretion and improved lift, which would benefit the wind power industry and the energy production under extreme weather conditions.

2. Methodology

2.1. Geometry and mesh

Numerical simulations were carried out on the NACA2412 airfoil section with a 1 m chord length to analyze the icing growth effect by varying LWC, angle of attack (AoA), and accretion time on a rectangular topological domain. Numerical simulation is performed by applying the computational fluid dynamics (CFD) software FENSAP-ICE, where the airflow is modeled, and the aerodynamic perfor-

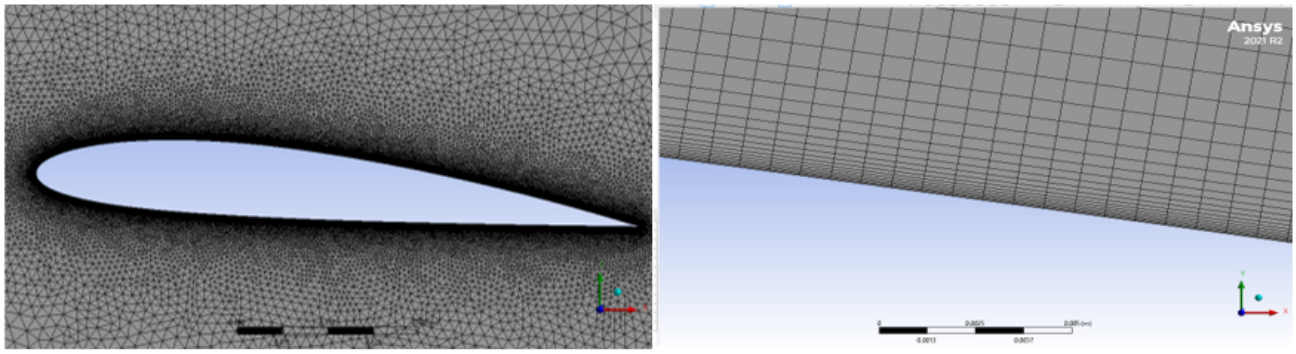

Figure 1. Meshing around the airfoil and the first layers enlarged

mance is evaluated for both bare and iced profiles. Unstructured (triangular) and semi-structured meshes were applied to the computational domain and the near wall region (airfoil). The resulting grid has elements within the boundary layer suitable for no-slip conditions around the airfoil. The no-slip boundary condition near the airfoil surface with a $y+$ value less than 1 is obtained using a Cadence calculator [21] because we will use a low-Re model. The first layer thickness is determined to be $1.43 \cdot 10^{-5}$ m, and 27 layers are inserted with growth rate of 1.08%, the growth rate in the domain of triangular mesh was set to 1.05% as shown in Fig. 1.

2.2. Flow conditions and boundary conditions

The density of air and droplets are set to be 1.394 kg/m^3 and 1000 kg/m^3, respectively, while the ice density was kept constant at 917 kg/m^3 with air static pressure set at 1013.25 hPa and air temperature of -20 °C, with -18 °C on the airfoil surface (wall). Boundary conditions are shown in Fig. 2. The flow conditions were set in the inlet to freestream velocity at 20 m/s, whereas to pressure coupled at 0 atm in the outlet. On the boundary domains top and bottom the command "symm" is applied to consider linear symmetry. The model describes continuous fluid motion involving phase properties changes (liquid to solid, i.e., water droplets in the airflow over the airfoil surface to ice formation). The numerical simulation predicts the accretion of ice on the blade surface by considering successive water droplet trajectories hitting the surface, followed by airflow calculation on the surface, and energy and mass conservation (heat balance) with the water droplets simulated over the object freezing. The water droplets simulated over the object may freeze or evaporate. The heat balance in the thermodynamic model includes droplet heating, and heat contained in the water flowing on the blade, convection, radiation and evaporation [22]. These conditions were considered

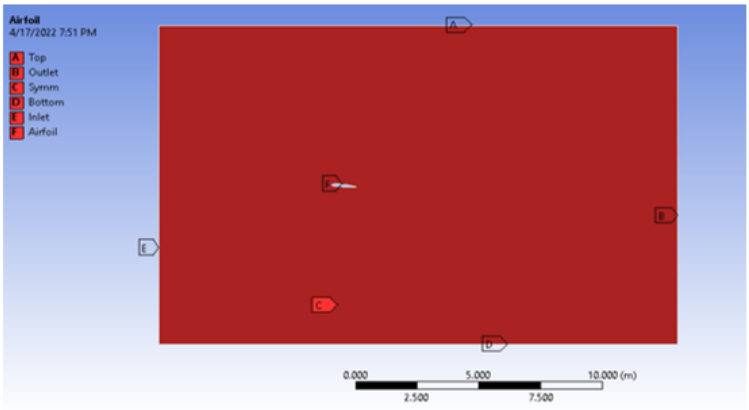

Figure 2. Boundary conditions on the rectangular computational domain

Table 1. Operating parameters of Airfoil NACA 2412

Parameter	Value
Temperature [°C]	-20
Velocity [m/s]	20
MVD [μm]	20
DSD	Langmuir D
LWC [g/m^3]	0.5; 1; 1.5
Exposure time [mins]	7; 20; 40; 60; 120; 180
AoA [°]	0; 5; 10; 15; 20

by the FENSAP ICE software. The turbulence model used is the k-ω SST model since it provides a better prediction of flow separation and exhibits less sensitivity to flow outside the boundary layer than other turbulence models. The effects of angle of attack, liquid water content (LWC), and accretion/exposure time on icing and the aerodynamic performance are simulated using FENSAP-ICE. The range of these parameters is shown in Table 1. The impact of size of the droplets hitting the accreting surface is important on the ice accretion. However, the range of droplet sizes that the Langmuir D distribution covers is relatively small; therefore, the consideration of this distribution in the model instead of the MVD had little effect on the ice accretion [23]. The parameters used in the study represented the normal working conditions experienced in real life scenario, with some being simplified to controlled natural environments though they vary from time to time such as LWC and temperature [24]. The droplets were assumed to be spherical, and the forces acting on the droplets were inertia and drag.

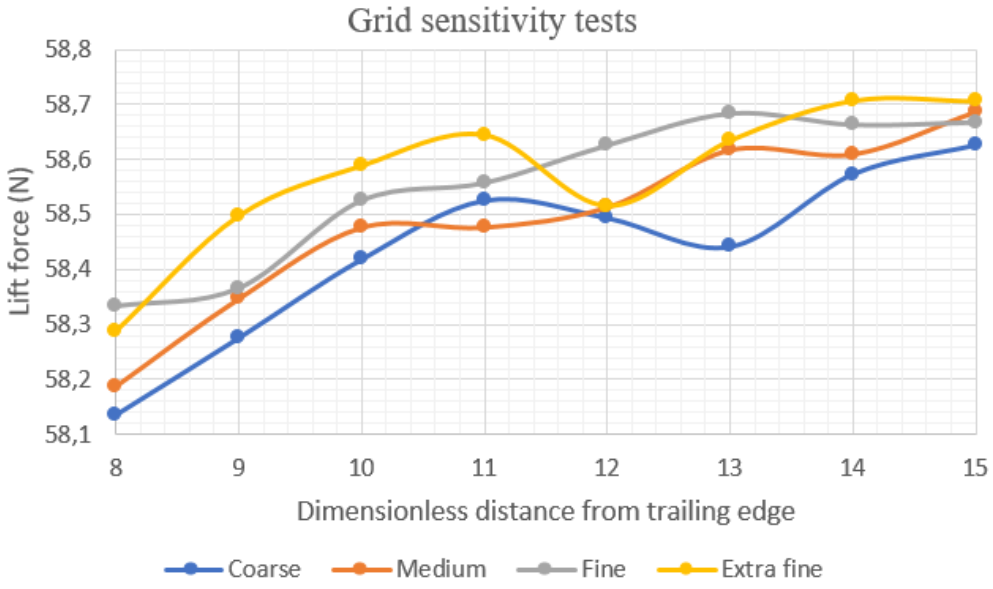

Figure 3. Mesh sensitivity analysis on Lift force (N) with varying lengths of computational domain behind airfoil trailing edge. The distance from the trailing edge is non-dimensionalized with the chord length

2.3. Grid independence and boundary sensitivity tests

Grid independence tests aim to obtain the optimal mesh and size of the computational domain considering accuracy and computational cost. The angle of attack had little impact on the mesh, the number of elements for fine mesh ranges from 502700 to 501710 for 0° to 20° AoA, respectively.

The grid sensitivity analysis is based on the aerodynamic performance by considering the lift force for varying lengths of computational domain behind the trailing edge. According to the analysis shown in Fig. 3, the distance behind the trailing edge does not significantly affect the lift force if it is within the recommended range, i.e., 10-15 times the chord length. The lift force obtained is between 58.15 N and 58.7 2N when the length of the computational domain behind the trailing edge varies between 8 and 15 times the chord length. The fine mesh was used with 14 m behind the trailing edge in the study since the value of lift force changed by 0.05% only when the size behind the trailing edge was increased from 14 m to 15 m.

3. Results and discussion

The effects of LWC, accretion time and angle of attack on ice mass and aerodynamic performance are examined.

3.1. Effects of LWC, accretion time and angle of attack on the mass of ice accretion

Mass of ice accreted was determined for accretion times of 7, 20, 40, 60,120 and 180 minutes, LWCs of 0.5 g/m^3, 1.0 g/m^3 and 1.5 g/m^3, and AoA of 0°, 5°, 10°, 15° and 20° (see Table 1). Figure 4 shows the effects of LWC, accretion time and angle of attack on the mass of ice accretion. Ice accretion is greatly affected by the angle of attack, with a lower angle causing the ice to accumulate mainly on the leading edge. In contrast, the higher angle of attack causes ice to accrete even at the trailing edge. The comparison shows the highest accretion mass at 10°, and the lowest at 20° angle of attack for all the LWCs considered. Ice accretion on the blade is also affected by the quantity of liquid water in the air. Increasing LWC means a higher amount of water in the atmosphere leading to a greater mass of ice accretion. Ice mass increases with LWC and increases exponentially with accretion time. The highest mass of ice obtained in 180 min is 3620 g at 10° and at 1.5 g/m^3 and the lowest mass is 940 g at 20° and at 0.5 g/m^3.

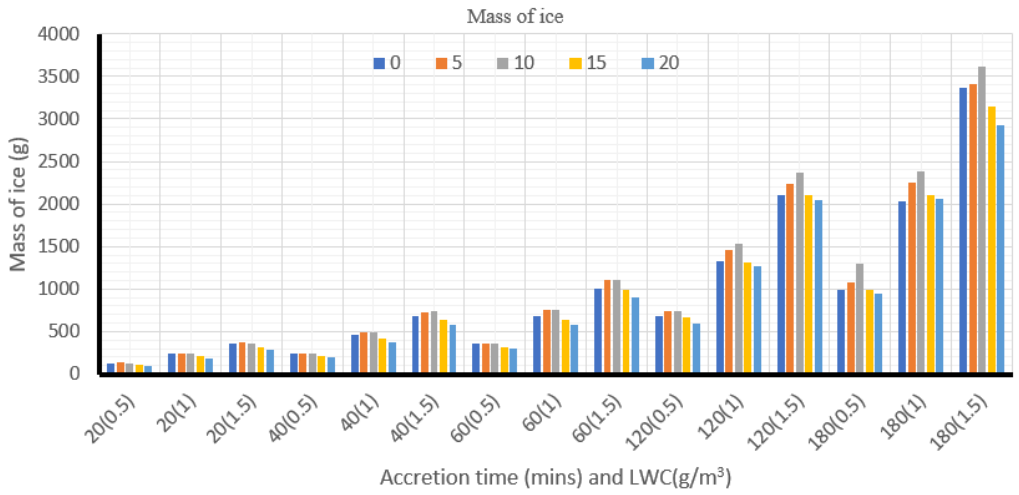

Figure 4. Effect of Liquid Water Content(g/m^3), accretion time (min) and angle of attack (°) on the mass of ice accretion (g)

3.2. Variation of CL/CD with accretion time

The aerodynamic performance of the airfoil will be evaluated via the ratio of lift and drag coefficients, CL/CD with Figure 5 showing the impact of ice accretion time. The CL/CD slightly increases before 20 minutes for angles of attack 10° and below due to increase in the stagnation point and airfoil shape from ice accretion distorting disturbance of flow distribution. This change is about 3.29%, 5.43%, and 1.48% for LWC of 0.5g/m^3, 1 g/m^3, and 1.5 g/m^3, respectively, for the 10° angle of attack. The comparison of the iced shapes in Figure 6 shows that ice on the leading edge raises the stagnation point after 20 minutes of accretion, enhancing the aerodynamic performance, which eventually degrades with further accretion. The highest CL/CD is 52.55, 53.65 and 51.63 for LWC of 0.5 g/m^3, 1 g/m^3 and 1.5 g/m^3, respectively, as it can be seen on the curve fitted on the data for 10° angle of attack. The CL/CD for small angle of attack between 0° to 10° increased slightly to about 20 minutes before it starts decreasing. For higher angle of attack (>10°), the CL/CD dropped immediately when ice started to accumulate on the surface, followed by a decreasing tendency. At 20° angle of attack, with minimal ice accretion on the surface after 20 minutes accretion, the CL/CD decreased by 53.38%, 57.41%, and 57.50% for LWC of 0.5 g/m^3, 1 g/m^3 and 1.5 g/m^3, respectively, as compared to the bare blade.

The ice accretion on the asymmetrical airfoil surface moves the stagnation point upward. Asymmetrical airfoils have a stagnation point slightly below the leading edge. Thus, with minimal icing on the surface, the stagnation point moves toward the upper surface, causing a slight increase in the CL/CD (see Fig. 5). Considering that the airfoil used in the study (NACA2412) had asymmetrical characteristics, the horizontal flow velocity hits the stagnation point slightly above the suction surface of the airfoil. Slight ice accretion on the surface raises the suction surface nearly to the stagnation

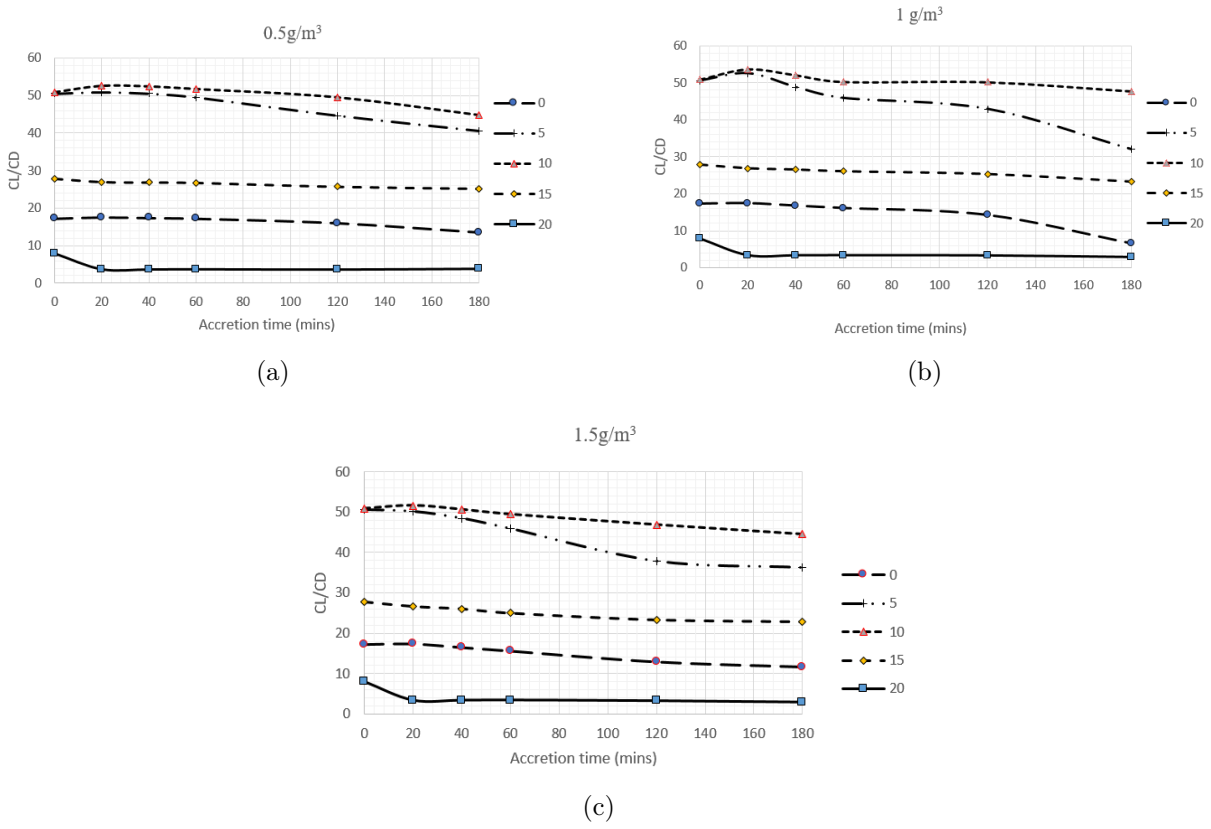

Figure 5. Variation of CL/CD with accretion time for different values of angle of attack and LWC

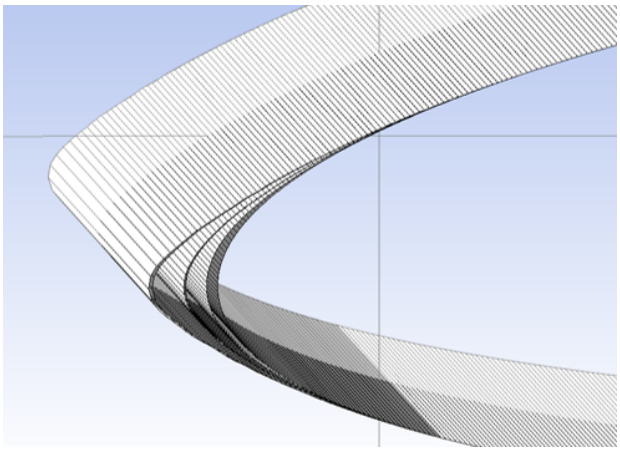

Figure 6. Accreted ice on the surface at 0°, 1 g/m^3 at 7,20 and 40 mins

point at lower accretion time and thus increases the CL/CD. According to the comparison presented on Fig. 6 for 0°, the accretion surface between the 7th and 40th minute shows that little change in the streamlines caused slight icing. Increasing angle of attack increment moves the stagnation point next to the suction surface and thus decreases the CL/CD.

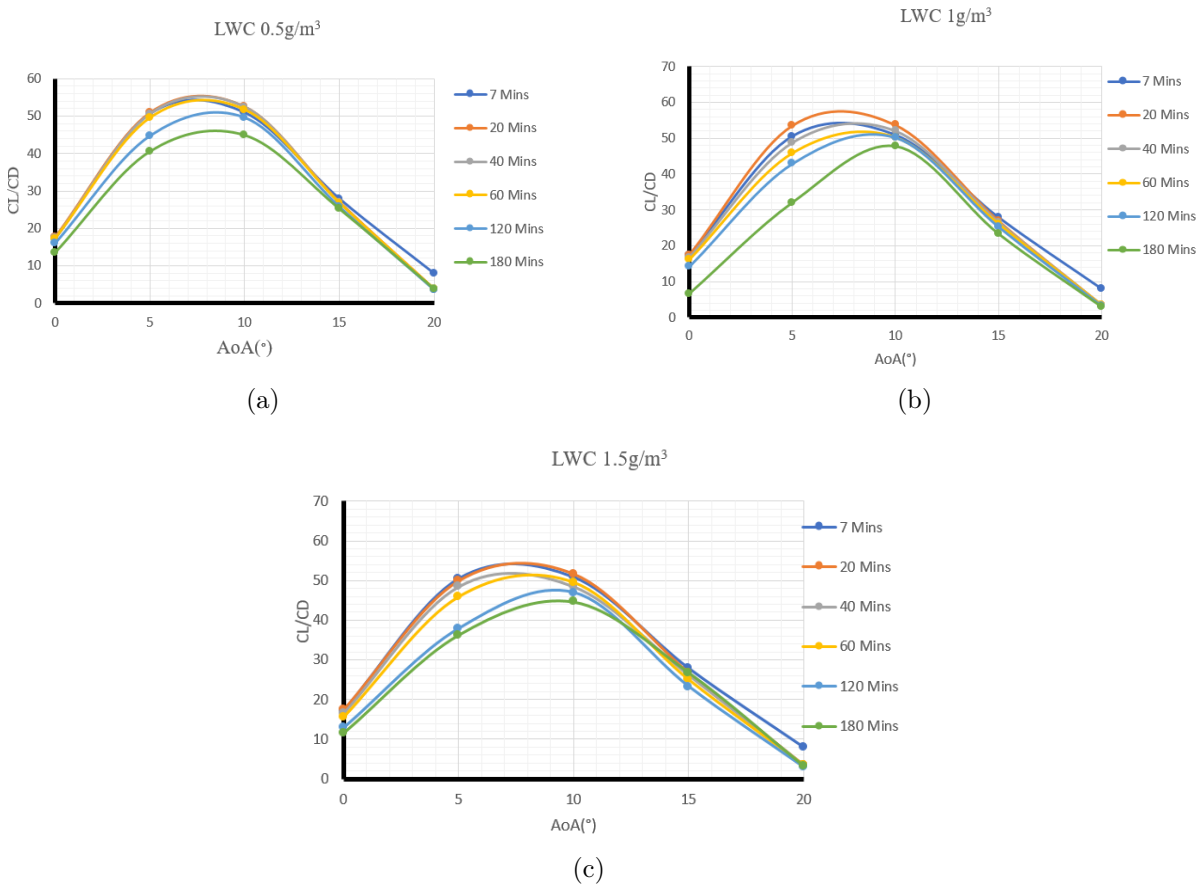

Figure 7. Variation of CL/CD with the angle of attack (°) for different values of accretion time (mins) and LWC (g/m^3)

3.3. Variation of CL/CD with the angle of attack

Fig. 7 shows the variation of CL/CD with the angle of attack for different accretion times and LWC. The ratio CL/CD for a bare airfoil is greatest for angles between 5° and 10°, and this tendency does not change for iced blades, but the value of this ratio is smaller for iced blades. This observation corresponds to those in [25]. Moreover, a greater decrease of CL/CD may be observed after a long accretion time for smaller values of angle of attack (below 10°). With the increase in LWC, more ice accumulation leads to greater CL/CD ratio reduction. The maximum of CL/CD is 53.52 for LWC of 0.5 g/m^3, whereas its highest value is 51.63 for 1.5 g/m^3.

3.4. Velocity distribution around an iced airfoil

The flow distribution over the airfoil is dependent on the angle of attack. At a lower angle of attack, the Kutta condition was met, while at a higher angle of attack, the separation zone moved upward towards the leading edge with vortices occurring at the trailing edge. Fig. 8 and 9 show the impacts of icing and varying angle of attack on the velocity distribution. Icing causes changes in airfoil shape, impacting on flow distribution, which can be observed due to the multi-shot simulations. Figure 8 shows the iced shapes at zero angle of attack, during the simulation of 3 hours accretion time and the impact caused by icing after the 3rd (minimal separation, 108 min) and the 5th shot (turbulent regions develop, 180 min) at LWC of 1.5 g/m^3. After further shots, the flow over the airfoil starts separating and causes some difficulty in the reattachment in the regions near the trailing edge, so that recirculation occurs.

Higher angle of attack led to vortices forming near the leading edge even for less amount of ice. The arrows near the trailing edge in Fig. 9 show the vortices in the recirculation region caused by the flow separation, and the vortices occur where arrows are missing. The backflow may influence droplet motion on the surface and freezing time, but further study is needed for a more profound description of this process.

4. Conclusions

The effects of ice accretion on the aerodynamic performance of an airfoil section have been examined under different ambient conditions. Icing of a NACA2412 airfoil was simulated numerically, and the lift and drag coefficients on the iced airfoil were calculated with varying LWC, accretion time and angle of attack. The aerodynamic performance was evaluated by comparing the ratio of lift and drag coefficients CL/CD obtained after different accretion times. The reduction of CL/CD was

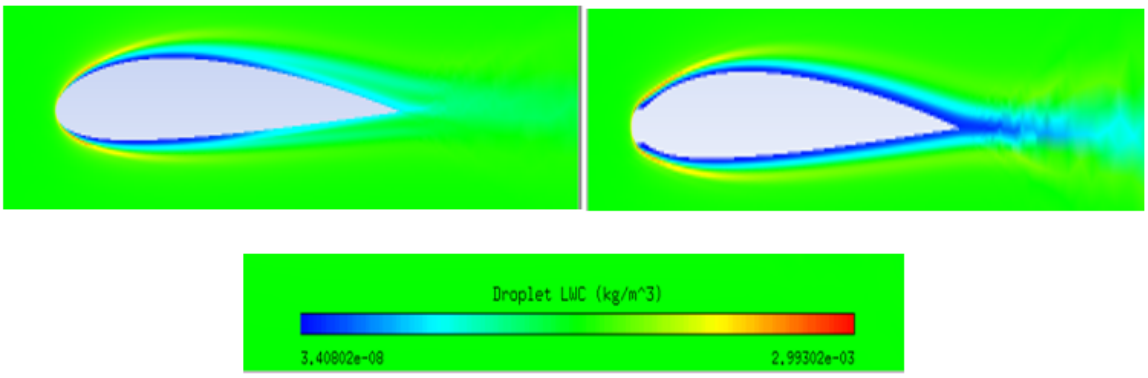

Figure 8. Effect of accretion time on ice shape and velocity distribution at 0° AoA and LWC of 1.5 g/m^3 in the simulation of 180 minutes accretion time at 3rd shot (108 min) and 5th shot (180 min)

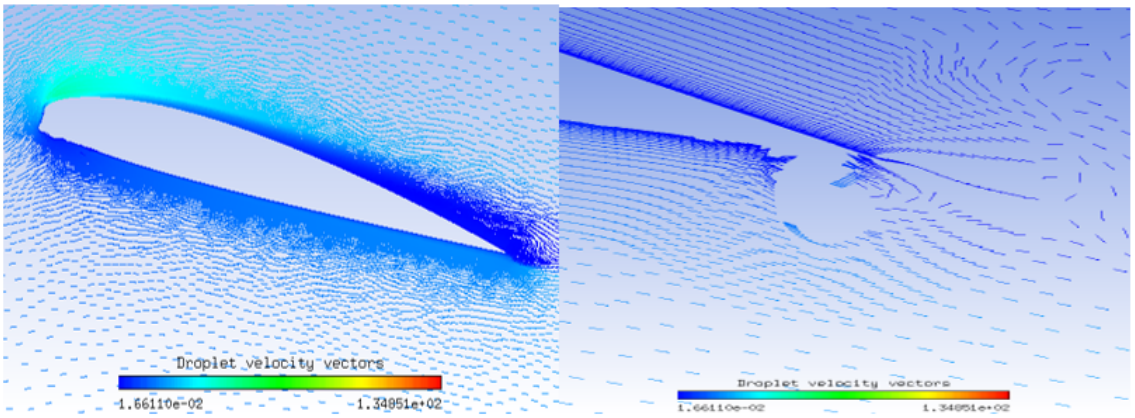

Figure 9. The flow distribution over the airfoil(left) and backflow (recirculation) at the trailing edge (right) at 10° AoA and LWC of 1.5 g/m^3

observed on the asymmetric shape of the airfoil after about 20 minutes of accretion time. However, a short enough accretion time, i.e. less than 20 minutes, may lead to a slight increase of the ratio CL/CD, because the stagnation point moves toward the upper surface making the airfoil to become more streamlined. LWC and angle of attack also influences the aerodynamic performance, mass of accreted ice and the velocity distribution over the airfoil surface. The higher LWC results in increased mass of accreted ice, and consequently, aerodynamic performance degradation. The mass of ice increased exponentially with accretion time. Increasing the angle of attack caused more ice to form on the lower surface and the flow separation region on the upper surface increased towards the leading edge. According to the results presented in the study, slight altering of the airfoil shape may increase aerodynamic performance making the wind turbine possible to work under adverse atmospheric conditions.

5. Acknowledgement

Project no. TKP2021-NVA-29 has been implemented with support from the Ministry of Innovation and Technology of Hungary from the National Research, Development and Innovation Fund, financed under the TKP2021-NVA funding scheme.

6. References

[1] N. Dalili, A. Edrisy, R. Carriveau, *A review of surface engineering issues critical to wind turbine performance*, Renewable and Sustainable Energy Reviews 13(2), 2009. pp. 428–438, CrossRef

[2] D.L. Johnson, R.J. Erhardt, *Projected impacts of climate change on wind energy density in the United States*, Renew Energy 85, 2016, pp. 66–73, CrossRef

[3] A.G. Kraj, E.L. Bibeau, *Phases of icing on wind turbine blades characterized by ice accumulation*, Renew Energy 35(5), 2010, pp. 966–972, CrossRef

[4] P. Blasco, J. Palacios, S. Schmitz, *Effect of icing roughness on wind turbine power production*, Wind Energy 20(4), 2017, pp. 601–617, CrossRef

[5] F. Afzal, M. S. Virk, *Review of Icing Effects on Wind Turbine in Cold Regions*, E3S Web of Conferences 72, 2018, p. 01007, CrossRef

[6] F. Martini, L.T. Contreras Montoya, A. Ilinca, *Review of Wind Turbine Icing Modelling Approaches*, Energies (Basel) 14(16), 2021, p. 5207, CrossRef

[7] A. Ilinca, *Analysis and Mitigation of Icing Effects on Wind Turbines*, in Wind Turbines, 2011, pp. 177–214, CrossRef

[8] J.G. Pallarol, B. Sunden, Z. Wu, *On Ice Accretion for Wind Turbines and Influence of Some Parameters*, In R. S. Amano & B. Sundén (Eds.), Aerodynamics of Wind Turbines: Emerging Topics, 2014, pp. 129–159, CrossRef

[9] L.T. Contreras Montoya, S. Lain, A. Ilinca, *A Review on the Estimation of Power Loss Due to Icing in Wind Turbines*, Energies (Basel) 15(3), 2022, p. 1083, CrossRef

[10] L. Gao, H. Hu, *Wind turbine icing characteristics and icing-induced power losses to utility-scale wind turbines*, Proceedings of the National Academy of Sciences 118(42), 2021, p. e2111461118, CrossRef

[11] M.C. Homola, M.S. Virk, P.J. Nicklasson, P.A. Sundsbø, *Performance losses due to ice accretion for a 5 MW wind turbine*, Wind Energy 15(3), 2012, pp. 379–389, CrossRef

[12] R. Luo, X. Chen, J. Guo, *Design of deicing device for wind turbine blade based on microwave and ultrasonic wave*, Journal of Physics: Conference Series 1748 (6), 2021, p. 062018, CrossRef

[13] O. Yirtici, I.H. Tuncer, S. Ozgen, *Ice Accretion Prediction on Wind Turbines and Consequent Power Losses*, Journal of Physics: Conference Series 753, 2016, p. 022022, CrossRef

[14] O. Yirtici, I.H. Tuncer, *Aerodynamic shape optimization of wind turbine blades for minimizing power production losses due to icing*, Cold Regions Science and Technology, 185, 2021, 103250, CrossRef

[15] X. Dong, D. Gao, J. Li, Z. Jincao, K. Zheng, *Blades icing identification model of wind turbines based on SCADA data*, Renew Energy 162, 2020, pp. 575–586, CrossRef

[16] L. E. Kollar, R. Mishra, *Inverse design of wind turbine blade sections for operation under icing conditions*, Energy Convers Management 180, 2019, pp. 844–858, CrossRef

[17] C. Montoya, L. Tatiana, S. Lain, A. Ilinca, A Review on the Estimation of Power Loss Due to Icing in Wind Turbines, Energies 15(3), 2022, CrossRef

[18] M.S. Virk, M.C. Homola, P.J. Nicklasson, *Relation Between Angle of Attack and Atmospheric Ice Accretion on Large Wind Turbine's Blade*, Wind Engineering 34(6), 2010, pp. 607–614, CrossRef

[19] P. Fu, M. Farzaneh, *A CFD approach for modeling the rime-ice accretion process on a horizontal-axis wind turbine*, Journal of Wind Engineering and Industrial Aerodynamics 98(4–5), 2010, pp. 181–188, CrossRef

[20] S. Hildebrandt, Q. Sun, *Evaluation of operational strategies on wind turbine power production during short icing events*, Journal of Wind Engineering and Industrial Aerodynamics 219, 2021, p. 104795, CrossRef

[21] *Compute Grid Spacing for a Given Y+*, Accessed May 02, 2022, CrossRef

[22] L. Makkonen, T. Laakso, M. Marjaniemi, K.J. Finstad, *Modelling and Prevention of Ice Accretion on Wind Turbines*, Wind Engineering 25(1), 2001, pp. 3–21, CrossRef

[23] *ANSYS FENSAP-ICE Tutorial Guide*, ANSYS 18.2. 2017, CrossRef

[24] L. E. Kollár, M. Farzaneh, *Modeling the evolution of droplet size distribution in two-phase flows*, International Journal of Multiphase Flow 33(11), 2007, pp. 1255–1270, CrossRef

[25] B. Csőre, L. Kollár, D. Fenyvesi, Jeges szárnyalak aerodinamikájának vizsgálata, Mérnöki és Informatikai Megoldások|Engineering and IT Solutions, 2022, I, pp. 19–27, CrossRef